A Dynamic Self-Healing System for Harmonic and Unbalanced Smart Microgrids Considering Renewable Energy Intermittency

Ontoseno Penangsang
Electrical Engineering Department, Faculty of Intelligent Electrical and Informatics Engineering, Sepuluh Nopember Institute of Technology, Surabaya, Indonesia
ontosenop@ee.its.ac.id

Rony Seto Wibowo
Electrical Engineering Department, Faculty of Intelligent Electrical and Informatics Engineering, Sepuluh Nopember Institute of Technology, Surabaya, Indonesia
ronyseto@ee.its.ac.id

Fysna Candra Pratama
Electrical Engineering Department, Faculty of Intelligent Electrical and Informatics Engineering, Sepuluh Nopember Institute of Technology, Surabaya, Indonesia
5022211101@student.its.ac.id (corresponding author)

Muhammad Rifad Faturrahman
Electrical Engineering Department, Faculty of Intelligent Electrical and Informatics Engineering, Sepuluh Nopember Institute of Technology, Surabaya, Indonesia
5022211043@student.its.ac.id

Tanazzaha Nur Izzati
Electrical Engineering Department, Faculty of Intelligent Electrical and Informatics Engineering, Sepuluh Nopember Institute of Technology, Surabaya, Indonesia
5022211001@student.its.ac.id

Received: 12 May 2025 | Revised: 21 June 2025, 11 July 2025, 20 July 2025, and 17 August 2025 | Accepted: 20 August 2025

 DOI: https://doi.org/10.48084/etasr.12080

ABSTRACT

This paper presents a dynamic, self-healing system for smart microgrids that addresses the harmonic distortion, voltage imbalance, and Renewable Energy Source (RES) intermittency using an Improved Whale Optimization Algorithm (IWOA). The IWOA simultaneously optimizes four equally weighted objectives — active power losses, voltage deviation, Total Harmonic Distortion (THD), and Phase Voltage Unbalance Rate (PVUR) — thereby overcoming the limitations of the conventional methods. An enhanced IWOA movement mechanism prevents the premature convergence in complex, unbalanced harmonic scenarios. When validated on a modified IEEE 33-bus system under diverse fault, load, and generation conditions, with realistic RES and harmonic modeling, the IWOA was found to significantly improve THD and PVUR compared to the conventional approaches. Furthermore, the IWOA outperforms the standard Whale Optimization Algorithm (WOA) by converging faster and providing a superior final solution, thus demonstrating its effectiveness in enhancing the microgrid resilience and power quality.

Keywords-IWOA; smart microgrids; dynamic self-healing; network reconfiguration; power quality; fault recovery

I. INTRODUCTION

Self-healing is a critical capability in modern power systems, providing the ability to automatically detect, diagnose and recover from disturbances without human involvement [1]. While effective in conventional grids, static self-healing strategies are inadequate for the dynamic and complex nature of decentralized networks [2]. Smart microgrids further increase the complexity due to the bidirectional power flows, high levels of Renewable Energy Sources (RES), and the widespread use of power electronics interfaces [3]. The variability of RES, such as solar and wind, increases the supply uncertainty, while single-phase and non-linear loads cause PVURs and harmonic distortion [4]. These challenges require dynamic self-healing frameworks that can adapt in real time while ensuring stability and power quality [5]. As the RES integration grows, maintaining the reliability under uncertain conditions becomes increasingly challenging [6]. The existing centralized control systems are not equipped to manage the frequent disturbances from the RES variability and the power quality issues, increasing the risk of instability, losses, and equipment degradation [7, 8]. Therefore, a real-time self-healing strategy involving network reconfiguration is essential in order to enhance the resilience, reduce the losses and maintain the voltage and power quality, particularly in the event of harmonic-rich and unbalanced loading. Various metaheuristic algorithms have been used for the Distribution Network Reconfiguration (DNR) problem to achieve a more resilient distribution network while maintaining optimal power quality. For instance, the Improved Bacterial Foraging with Simulated Annealing (IBSA) algorithm [9] effectively improved the voltage profile and reduced the power losses in the IEEE 30- and 33-bus systems. However, it failed to address power quality indices, such as THD and PVUR. Similarly, the Improved Hybrid Particle Swarm Optimization (IHPSO) algorithm [10] produced better results for the voltage and THD on the IEEE 33-bus system, but overlooked the dynamic reconfiguration and PVUR considerations. WOA [11] successfully reduces the power losses and enhances the voltage profiles, but does not address multi-objective considerations or real-time disturbance adaptability. As presented in Table I, most existing methods fail to address harmonic distortion and PVUR simultaneously, and none implement a fully dynamic self-healing mechanism that responds to real-time variations. To address these issues, this study proposes an enhanced WOA-based self-healing strategy. Although the standard WOA is simple, it converges slowly and tends to stagnate, particularly in non-linear, high-dimensional scenarios, such as real-time self-healing in active distribution networks [12, 13]. This study proposes an IWOA to overcome the limitations of the conventional WOA and improve self-healing in modern distribution networks. Although the standard WOA is computationally efficient, it is limited to addressing two objectives (typically power losses and the voltage profile) and often suffers from premature convergence, particularly in nonlinear and unbalanced conditions involving harmonic distortion. The proposed IWOA overcomes these limitations by applying an equality-based weight-sum approach to optimize four critical objectives simultaneously: power losses, voltage deviation, THD and PVUR. This balanced formulation ensures a comprehensive power quality and operational improvement. Additionally, the IWOA improves the search performance by dynamically adjusting the contraction behavior of the control vector to enhance exploration and prevent falling into local optima. This modification is particularly effective in dynamic self-healing scenarios involving unbalanced harmonics, in which the standard WOA performs poorly. The algorithm has been validated using a modified IEEE 33-bus system under various contingencies at peak load and generation.

TABLE I. OVERVIEW OF RELATED WORKS ON OPTIMIZATION ALGORITHMS FOR DISTRIBUTION NETWORK RECONFIGURATION

Ref.	Optimization algorithm	Test system	Voltage profile	Power losses	THD	PVUR	Dynamic system
[9]	IBSA	IEEE 30 bus, IEEE 33 bus	✓	✓	-	-	✓
[10]	IHPSO	IEEE 33 bus	✓	✓	✓	-	✓
[11]	WOA	IEEE 33 bus, IEEE 69 bus	✓	✓	-	-	-
[14]	PSO	IEEE 33 bus	✓	✓	-	-	-
[15]	IMODBO	IEEE 33 bus, IEEE 69 bus	✓	✓	-	-	✓
Proposed method	IWOA, WOA	Modified IEEE 33 bus	✓	✓	✓	✓	✓

II. PROBLEM FORMULATION

This study optimizes switch combinations with the objective of enhancing the microgrid reliability and resilience after a fault. In order to ensure high-quality power, the system compares two multi-objective functions:

- Conventional objective: aiming to minimize the power loss and regulate the voltage.
- Proposed objective: aiming to reduce PVUR and manage THD, in addition to minimizing the losses and regulating the voltage.

In order to assess the system's state and the efficacy of the reconfiguration strategies under both conventional and proposed objective functions, the following Key Performance Indicators (KPIs) [16] were used:

- Minimizing harmonics (F_1) by enhancing the power quality through the control of the harmonic distortion levels. The objective function is formulated to penalize any violation of the permissible THD limits:

$$F_1 = min\ (\prod_i^{nbus} PFTHD_i) \quad (1)$$

$$PFTHD_i = \begin{cases} 1 \; if, \; THD_i \leq 5 \\ exp\,(\frac{THD_i}{5})^{0.8}, for\ others \end{cases} \quad (2)$$

where N_{bus} is the total number of buses in the system, the penalty factor for THD at bus i ($PFTHD_i$) is defined according to the IEEE-519 2022 standard, which sets the THD limit at 5%, THD_i is the harmonic distortion at bus i, calculated as the ratio of the RMS value of the harmonic components to the RMS value of the fundamental voltage, and is expressed as a percentage (%), and $exp\,(\frac{THD_i}{5})^{0.8}$ is a penalty coefficient that increases when THD exceeds the standard, helping the optimizer find solutions within acceptable harmonic limits.

- Minimizing PVUR (F_2) by ensuring the maintenance of the voltage balance among the three phases (R, S, T), which is defined by the IEEE Standard 141-1993 as the ratio of the negative to positive sequence voltage components. The allowable PVUR limit is 2%:

$$F_2 = min\,(\prod_i^{nbus} PFPVUR_i) \quad (3)$$

$$PFPVUR_i = \begin{cases} 1\,, if\ PVUR_i \leq 2 \\ exp\,(\frac{PVUR_i}{2})^{\beta}, for\ others \end{cases} \quad (4)$$

where the penalty factor for the PVUR ($PFPVUR_i$) is the deviation from the standard limit at each bus i, $PVUR_i$ is the PVUR at bus i, expressed as a percentage (%), and β is a user-defined penalty coefficient (e.g., 0.8) that determines the severity of the penalty applied when the PVUR exceeds the permissible limit.

- Maintaining the voltage levels (F_3) at all buses by remaining within the acceptable range of 0.95-1.05 per unit, thereby facilitating the stable system operation:

$$F_3 = min\,(\prod_i^{nbus} PFV_i) \quad (5)$$

$$PFV_i = \begin{cases} |\,1 - V_i\,|\,, if\ 0.95 \leq 1.05 \\ exp\,(\alpha\,|\,1 - V_i\,|), for\ others \end{cases} \quad (6)$$

where PFV_i is the penalty factor of the voltage in each phase with V_i voltage.

- Minimizing the active power losses (F_4) by improving the power quality:

$$F_4 = min\,(P_{loss}) \quad (7)$$

where P_{losses} is the sum of the active power losses across all branches of the network. The smaller the value of this variable is, the more optimized is the result.

To handle multiple performance goals at once, a normalized weighted-sum method is used to form the overall objective function. Each objective is scaled by its base-case value to ensure a balanced contribution and eliminate the differences in units:

$$F_{obj} = \frac{F_1}{F_{1,base}} + \frac{F_2}{F_{2,base}} + \frac{F_3}{F_{3,base}} + \frac{F_4}{F_{4,base}} \quad (8)$$

A multi-objective optimization strategy was developed to minimize the four KPIs: power losses, THD, PVUR, and voltage deviation. Figure 1 shows the weight distribution, with each corner corresponding to a single-objective case. The present study uses an equal-weight approach to balance all KPIs (compromise Solution, red star). Each objective, F_n, is normalized by its base-case value, $F_{n,base}$ [17], ensuring that all KPIs are treated with equal importance.

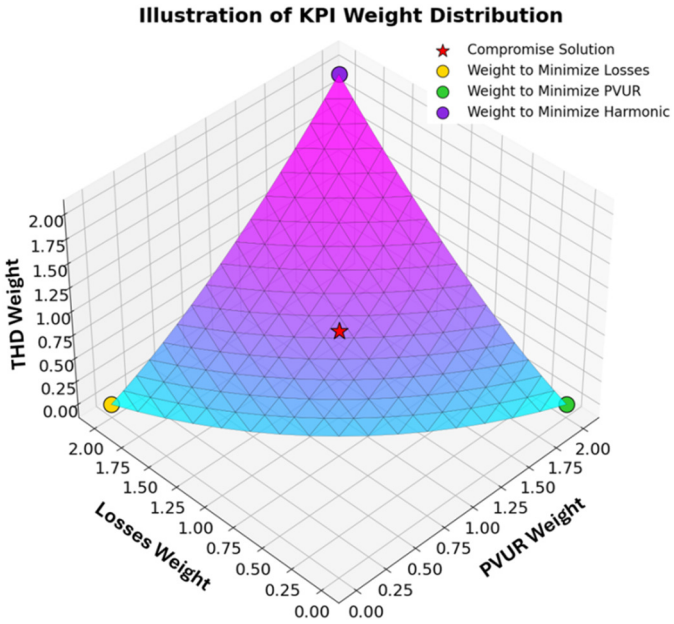

Fig. 1. Weight distribution of multi-objective KPI.

III. WHALE OPTIMIZATION ALGORITHM

Authors in [18] proposed the WOA, which is inspired by the hunting behavior of humpback whales. The algorithm models the whales' movements in three phases: searching, encircling prey, and the bubble-net attack method (the exploitation phase) [19]:

- Searching and encircling the prey

$$D = \left|\vec{C}\,\vec{X}_{rand} - \vec{X}\right| \quad (9)$$

$$\vec{X}(t+1) = \vec{X}_{rand} - \vec{A}\vec{D} \quad (10)$$

where D is the distance between the current population optimal individual and other individuals, $\vec{X}_{rand}$ is the random whales in current iteration, and $X(t+1)$ is the location of the next generation population individual. The encircling phase is:

$$\vec{D} = \left|\vec{C}\vec{X}^*(t) - \vec{X}(t)\right| \quad (11)$$

$$\vec{X}(t+1) = \vec{X}^*(t) - \vec{A}\vec{D} \quad (12)$$

where $X^*$is the best position vector, $\vec{X}$ is the position vector with coefficient vector, $\vec{X}^*(t)$ is the location of the optimal candidate solution, and $\vec{X}(t)$ is the location of the current population individual. The position update formula is:

$$\vec{A} = 2\vec{a} \cdot \vec{r} - \vec{a} \quad (13)$$

$$\vec{C} = 2 \cdot \vec{r} \quad (14)$$

$$a = 2 * \left(1 - \frac{t_{iter}}{Tmax}\right) \quad (15)$$

where $\vec{A}$ is convergence vector, $\vec{C}$ is the oscillation vector within $\vec{a}$ that linearly decreases from 2 to 0, and $\vec{r}$ is a random number between (0,1).

- Bubble-net attacking method (exploitation phase)

$$X(t+1) = \begin{cases} X^*(t) - \vec{A}\vec{D}, & if\ p < 0.5 \\ \vec{D}e^{bl}\cos 2\pi l + X^*(t), & if\ p \geq 5 \end{cases} \quad (16)$$

where, b is a constant that describes the spiral shape, p is a random position between (0,1), and l is between (-1,1).

IV. PROPOSED METHOD

To overcome the limitations of the standard WOA [20] in the dynamic self-healing of smart microgrids with RES, the study introduces IWOA [21], which addresses key challenges, such as harmonic imbalance, PVUR, voltage deviation, and power loss under changing conditions, and handles discrete reconfiguration. The linear vector movement mechanism is modified to prevent the premature convergence and support solution mapping [22, 23].

A. Adaptive Convergence Factor

In standard WOA, the convergence factor decreases linearly from 2 to 0, which can result in an imbalanced exploration-exploitation ratio. This study aims to improve this by using a nonlinear adaptive approach to avoid the premature convergence and enhance the search performance:

$$a = 2\left(1 - \left(\frac{t_{iter}}{T_{max}}\right)^3\right) \quad (17)$$

This formulation allows a to gradually decrease in the early iterations, which promotes a wider global search of the solution space. In the later stages, it decreases more rapidly to intensify the local search and refine the best-found solutions, as depicted in Figure 2.

B. Modified Position Update Equations

To further refine the balance between the exploration (searching for prey) and exploitation (encircling and attacking the prey), the position update equations are modified by introducing a control parameter, w, acting as an inertial weight that modulates the step size of the whale's movement:

- exploration phase (search for prey, if $|A| \geq 1$

$$\vec{X}(t+1) = \vec{X}_{rand} - (w \times \vec{A}\vec{D}) \quad (18)$$

- exploitation phase (shrinking encircling, if $|A| < 1\ and\ if\ p < 0.5$

$$\vec{X}(t+1) = \vec{X}^*(t) - \left(w \times \left(\vec{A}\vec{D}\right)\right) \quad (19)$$

- exploitation phase (shrinking encircling, if $|A| < 1\ and\ if\ p \geq 0.5$

$$\vec{X}(t+1) = \left(w \times \vec{D}e^{bl}\cos 2\pi l + X^*(t)\right) \quad (20)$$

It is important to note that w is a control parameter that regulates the balance between the exploration and exploitation during the algorithm's iterations, rather than a weight in the combined objective function. The weight values in the objective function can be adjusted to reflect the desired power quality solution. A higher weight results in a greater influence on the objective, while a lower weight has less impact. In this study, equal weights are used for the sum of objectives to achieve an optimal solution for each individual objective function.

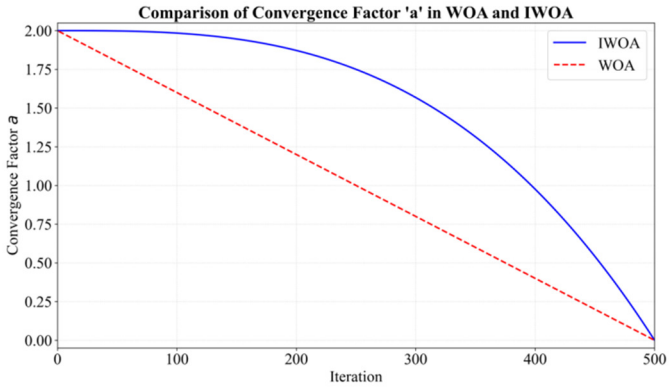

Fig. 2. Comparison of convergence factor a between WOA and IWOA.

C. Discretization of Continuous Solutions

IWOA operates within a continuous search space, whereas network reconfiguration is a discrete problem involving switches that are either open or closed. A mapping function is used to convert the continuous position of each whale into a valid switch configuration. For each dimension d, the nearest valid switch state from the discrete set S_d is chosen:

$$m_d = \arg \min_{z \epsilon S_d} |x - c_d| \quad \forall d \in \{1,2,\dots,dim\} \quad (21)$$

where d is the number of dimensions, S_d is the discrete search space, and c_d is the position in the continuous space. The corresponding discretized position m_d is the closest value in S_d to c_d, and the flowchart of the IWOA is portrayed in Figure 3. The main procedure for applying the proposed IWOA is given with the pseudocode:

```
Pseudocode of IWOA:
Input:
N - Number of Whale agents
Tmax - Maximum iterations
dim - Number - Decision variables
Sd - Search Space
W - Control weight
B - Spiral Constant
Fitness - Objective function
Output:
X_best - Best position
F_best - Best fitness
Step 1: Initialization
1: initialize Xi random in Sd
2: Fi ← Fobj(Xi)
3: X_best ← argmin Fi, F_best ← min(Fi)
4: t ← 1
```

```
Step 2: Main Iteration Loop
5: While t ≤ Tmax do
6:   Compute control coefficient:
7:    a = 2 * (1 - (t / Tmax)^3)
8:   For i = 1 to N do:
9:    Generate r ∈ [0,1], p ∈ [0,1], l ∈
[-1,1]
10:   Compute:
11:   A= 2 * a * r - a
12:   C = 2 * r
13:   If p < 0.5 then
14:    If |A| < 1 then
15:   //Shrink encircle - exploit
16:   D = |C * X_best - X_i|
17:   X_new = X_best - w * A * D
18:    Else
19:   //Explore: pick X_rand
20:   Pick X_rand from population
21:   D = |C * X_rand - X_i|
22:   X_new = X_rand - w * A * D
23:    EndIf
24:  Else
25:    // Spiral bubble-net attack
26:    D = |X_best - X_i|
27:    X_new = w * D * exp(b * l) *
cos(2πl) + X_best
28:  EndIf
29:  //Map X_new to nearest discrete   per
dim
30:  For d = 1 to dim:
31: X_new[d] = argmin_z∈Sd |X_new[d] - z|
32:   EndFor
33:   Evaluate new fitness F_i_new ←
Fobj(X_new)
34:   If F_i_new < F_i then
35:      X_i ← X_new
36:      F_i ← F_i_new
37:   EndIf
38:   If F_i_new < F_best then
39:      X_best ← X_new
40:      F_best ← F_i_new
41:   EndIf
42:  EndFor
43:  t ← t + 1
44: EndWhile
Step 3: Return Result
44: Return X_best, F_best37: F_best ←
F_i_new
38:         EndIf
39:     EndFor
40:     t ← t + 1
41: EndWhile
Step 3: Return Result
42: Return X_best, F_best
```

The IWOA pseudocode enables multi-objective optimisation of dynamic self-healing in smart microgrids, updating the whale positions with an adaptive convergence factor that balances the exploration and exploitation. Each solution is mapped to a discrete switch configuration and evaluated based othe n power losses, voltage deviation, THD, and PVUR. This iterative process converges on an optimal reconfiguration, thus enhancing the power quality and improving the system resilience under fault conditions.

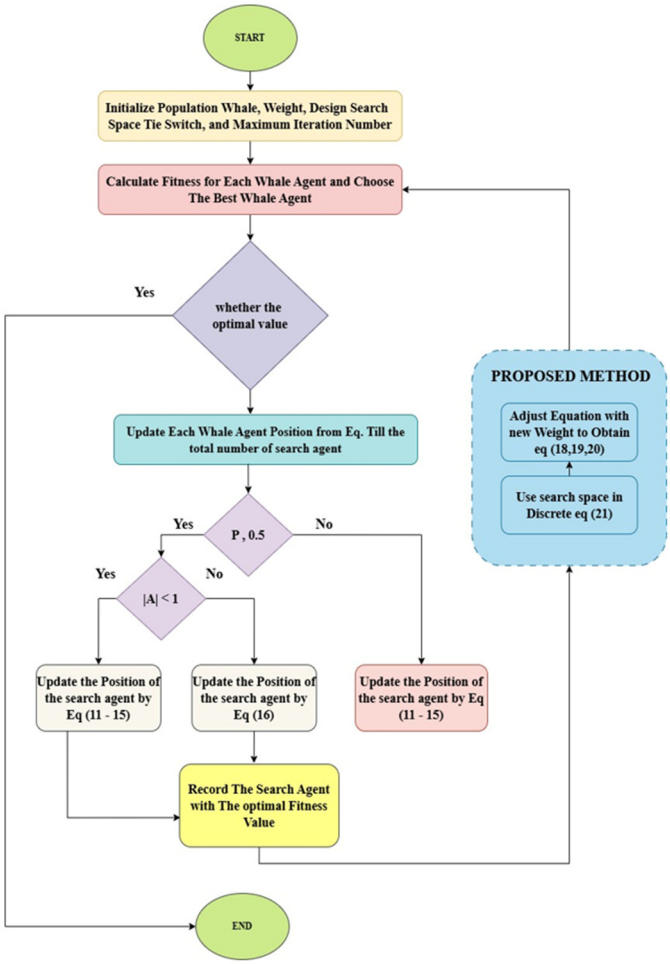

Fig. 3. IWOA flowchart for network reconfiguration.

V. DYNAMIC SELF-HEALING SYSTEM MODELING

The proposed framework was evaluated using a modified IEEE 33-bus system containing four microgrids, as presented in Figure 4. The reliability was ensured by running 50 repetitions of each scenario with 50 agents, using unbalanced loads, time-varying renewable generation, and harmonic data to simulate realistic dynamic and fault conditions.

A. Renewable Energy Profile

Figure 5 displays the output patterns of the Photovoltaic (PV) and wind energy. The PV output typically follows a diurnal curve, whereas the wind generated energy fluctuates irregularly due to its unpredictable nature. These profiles simulate RES intermittency, which poses significant challenges for real-time self-healing.

B. Unbalanced Load Profile and Distributed Generators

The imbalances in load and generation, caused by uneven single-phase connections and RES injection, affect the voltage quality and increase the losses. This study models unbalanced loads and a combination of single-phase and three-phase RES across phases R, S, and T, as shown in Figure 6 and Table II.

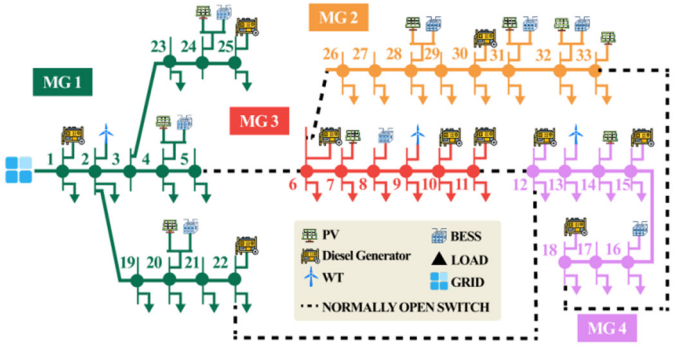

Fig. 4. Modified IEEE 33-bus multi-area test system with high renewable energy penetration.

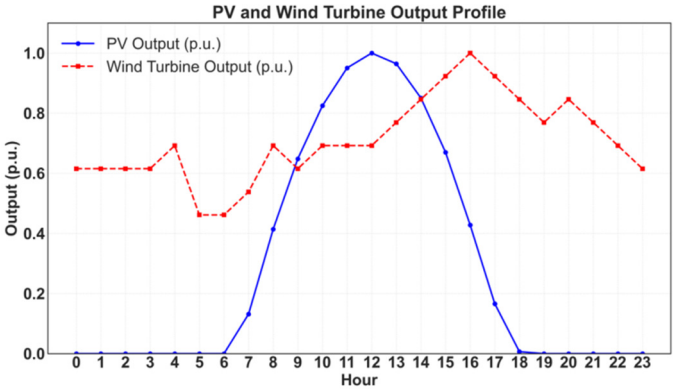

Fig. 5. Hourly power output profile of solar PV and wind turbine generation in per-unit (p.u.) values.

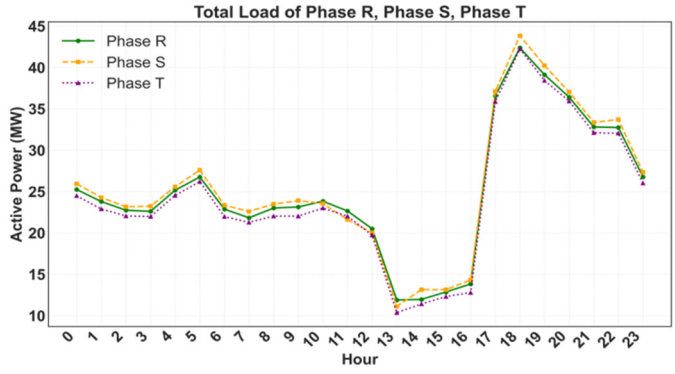

Fig. 6. Hourly active power load profile (MW) for phases R, S, and T over a 24-hour period.

Figure 7 presents the 24-hour aggregate R, S, T phase generation that supplies the load, with the output displaying a balanced state, exhibiting minor imbalances from the single-phase units. The peak is observed at 13:00, which is characterized by phase S due to the presence of concentrated single-phase sources. This phenomenon underscores the considerable influence of the solar PV energy during the period of peak sunlight.

TABLE II. TYPE AND NUMBER OF ENERGY RESOURCES

Sources	Phase type	MG 1	MG 2	MG 3	MG4
PV	1 Phase	3	3	0	0
	3 Phase	0	0	1	1
Wind turbine	1 Phase	1	1	0	0
	3 Phase	3	3	0	0
BESS	1 Phase	0	0	1	1
	3 Phase	3	0	3	3
Distributed generator	3 Phase	0	1	0	0

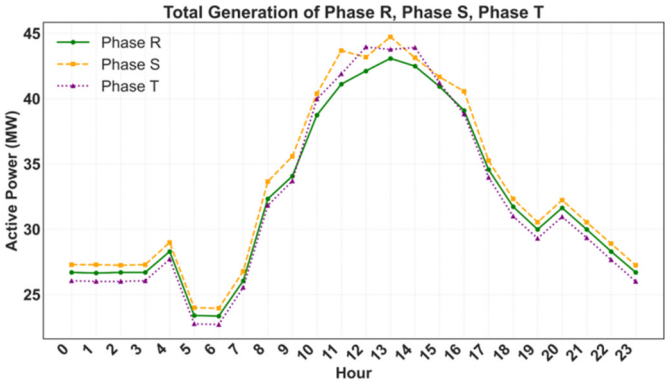

Fig. 7. Hourly active power generation profile (MW) for phases R, S, and T over a 24-hour period.

C. Harmonic Profile

It was found that harmonic distortion increased under unbalanced conditions with inverter-based RES. Figure 8 shows that phase T exhibits the highest THD, attributable to the uneven distribution of single-phase inverters, particularly during the period of peak solar irradiation.

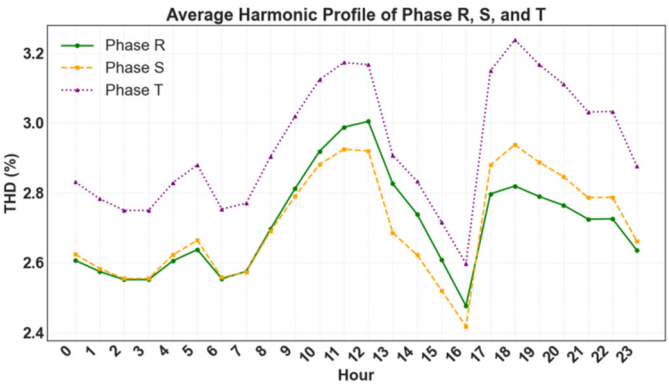

Fig. 8. Hourly average THD (%) for phases R, S, and T over a 24-hour period.

VI. RESULTS AND DISCUSSION

The performed analysis compares the WOA and IWOA using both conventional and proposed optimization approaches during three fault scenarios: N-1, N-2, and N-3 contingencies. In addition, the flexibility of the proposed multi-objective framework is validated through a weight sensitivity analysis,

which explores the performance trade-offs associated with different objective priorities.

A. Weight Sensitivity Analysis

The IWOA framework's flexibility was assessed through a weight sensitivity analysis, prioritizing individual objectives and comparing them with a balanced, equal-weight strategy, as illustrated in Figure 9. Prioritizing a single objective can enhance that specific metric while concomitantly causing substantial deterioration in other areas: voltage regulation, doubled the PVUR.

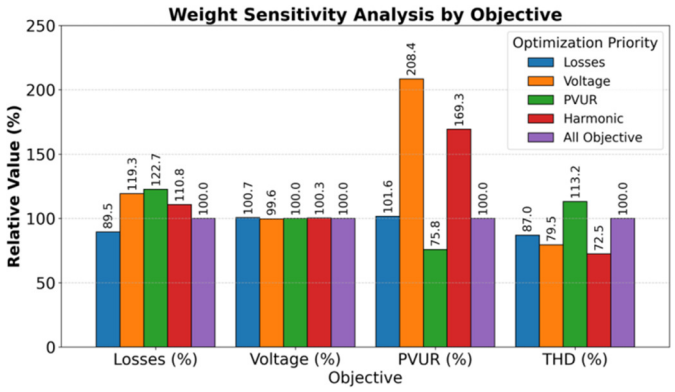

Fig. 9. An analysis of performance trade-offs between prioritizing a single metric and a balanced strategy.

This finding indicates that single-objective optimization can result in imbalanced system-wide performance. The analysis confirms that the balanced "all objective" approach provides the most effective solution by preventing the extreme negative outcomes in any single category. This underscores the importance of a multi-objective strategy to effectively address the intricate, interrelated challenges inherent in contemporary smart microgrids.

B. Single Line Fault During Peak Generation (N-1)

An assessment of the system restoration after a single line fault during peak PV generation revealed that all strategies successfully restored the power, as shown in Table III. The conventional objectives, including both WOA and IWOA, resulted in a suboptimal power quality, with the maximum THD exceeding 7%. The adoption of the proposed objectives, including PVUR and THD, resulted in a substantial enhancement of the power quality. The maximum THD decreased to approximately 4.0% - 4.2%, and the maximum PVUR was reduced to 1.274%. However, this increase was balanced by a simultaneous rise in the power losses, which reached 0.249 MW. A comparison of the algorithms revealed that IWOA demonstrates superior performance: while the losses were equivalent, IWOA exhibited a reduced maximum THD (4.007% compared to 4.183% for WOA) and a superior average power quality overall. This finding underscores the IWOA's enhanced ability to navigate complex solution spaces and identify more refined, high-quality operational configurations for the microgrid.

C. Two Line Fault During Peak Load (N-2)

This study evaluates the phenomenon of self-healing in the context of a severe N-2 contingency during the peak load. Table IV presents the findings, demonstrating that all strategies successfully restored the power after the initial outage. Under conventional objectives, the power quality was suboptimal, with maximum THD reaching 7.295%. The proposed objectives, incorporating power quality metrics, led to a substantial improvement in performance: IWOA reduced the maximum THD to 4.139% and WOA to 4.512%. This reduction in power quality was followed by a slight increase in the power losses (IWOA: 0.121 MW, WOA: 0.118 MW), indicating a trade-off between the power quality and loss minimization. A comparison of the proposed methods reveals that the IWOA delivered a superior overall power quality. Despite its slightly higher losses, IWOA achieved a lower maximum THD (4.139% versus 4.512%) and a lower maximum PV unbalance rate (1.274% versus 1.354%) than the standard WOA. A marginal increase in losses when compared to WOA (proposed, 0.121 MW versus 0.118 MW) was observed in IWOA (proposed), yet it demonstrated a superior overall power quality by achieving lower max PVUR (1.274% versus 1.354%), lower avg PVUR (0.611% versus 0.775%), lower max THD (4.139% versus 4.512%), and lower avg THD (2.230% versus 2.260%).

TABLE III. PERFORMANCE COMPARISON OF WOA AND IWOA UNDER N-1 FAULT (LINE 5) AT PEAK GENERATION AFTER NETWORK RECONFIGURATION

Method	Disconnected switch	Min volt (p.u)	Max volt (p.u)	Avg volt (p.u)	Min THD (%)	Max THD (%)	Avg THD (%)	Min PVUR (%)	Max PVUR (%)	Avg PVUR (%)	Losses (MW)	Outage busses (unit)
Before recovery	33, 34, 35, 36, 37	0 (Power outage)	1.02	0.365 (Power outage)	0 (Power outage)	1.025	0.181 (Power outage)	0 (Power outage)	1.779	0.654 (Power outage)	0.075	21
IWOA (prop.)	11, 14, 32, 27	0.998	1.024	1.011	0.192	4.007	2.318	0.015	1.274	0.611	0.249	0
WOA (prop.)	33, 34, 36, 25	0.999	1.024	1.013	0.186	4.183	2.447	0.013	1.274	0.622	0.249	0
IWOA (conv.l)	35, 12, 15, 27	0.999	1.023	1.011	0.243	7.067	3.83	0.017	2.609	1.159	0.219	0
WOA (conv.)	8, 14, 15, 27	0.998	1.026	1.011	0.264	7.841	4.148	0.018	2.611	1.173	0.221	0

D. Three Line Fault During Lowest VRE Generation (N-3)

This study investigates the system's capacity for self-healing in the context of an extreme N-3 contingency, precipitated by a scenario of limited renewable energy generation. Table V presents the outcome of each strategy, indicating the restoration of full service following the initial outage. The conventional objectives were met, with low power losses (as low as 0.082 MW) being achieved; however, this led to severe power quality problems, with maximum PVUR at 4.244% and THD at 4.690%. The proposed objectives resulted in a substantial enhancement of the power quality, with a

reduction in the maximum PVUR to approximately 1.2-1.3% and THD to around 3.0-3.5%. This improvement, however, was followed by a significant increase in the power losses, which reached 0.183 MW for IWOA and 0.196 MW for WOA. A direct comparison using the proposed framework revealed that the IWOA offered a more balanced and effective solution. The experimental model demonstrated a reduction in the power losses (0.183 MW versus 0.196 MW) and a lower maximum PVUR (1.238% versus 1.293%) compared to the standard WOA. These findings indicate its superior performance under extreme fault conditions.

TABLE IV. PERFORMANCE COMPARISON OF WOA AND IWOA UNDER N-2 FAULT (LINES 6 AND 26) AT PEAK LOAD AFTER NETWORK RECONFIGURATION

Method	Disconnected switch	Min volt (p.u)	Max volt (p.u)	Avg volt (p.u)	Min THD (%)	Max THD (%)	Avg THD (%)	Min PVUR (%)	Max PVUR (%)	Avg PVUR (%)	Losses (MW)	Outage busses (unit)
Before recovery	33, 34, 35, 36, 37	0 (Power outage)	1.017	0.425 (Power outage)	0 (Power outage)	0.57	0.126 (Power outage)	0 (Power outage)	1.672	0.052 (Power outage)	0.06	19
IWOA (prop.)	35, 14, 36	0.995	1.015	1.004	0.186	4.139	2.23	0.0147	1.274	0.6109	0.121	0
WOA (prop.)	10, 34, 36	0.996	1.014	1.004	0.186	4.512	2.26	0.0198	1.354	0.775	0.118	0
IWOA (conv.)	10, 25, 34	0.995	1.013	1.006	0.179	7.2954	3.903	0.016	2.608	1.158	0.113	0
WOA (conv.)	10, 22, 25, 34	0.98	1.01	0.998	0.149	5.8263	3.49	0.018	2.611	1.173	0.115	0

TABLE V. PERFORMANCE COMPARISON FOR N-3 FAULT (LINES 6, 12, 26) AT LOWEST VRE GENERATION POST-RECONFIGURATION

Method	Disconnected switch	Min volt (p.u)	Max volt (p.u)	Avg volt (p.u)	Min THD (%)	Max THD (%)	Avg THD (%)	Min PVUR (%)	Max PVUR (%)	Avg PVUR (%)	Losses (MW)	Outage busses (unit)
Before recovery	33, 34, 35, 36, 37	0 (Power outage)	1.017	0.425	0 (Power outage)	0.57	0.126 (Power outage)	0 (Power outage)	1.672	0.52 (Power outage)	0.06	19
IWOA (prop.)	35, 36	0.998	1.01	1.003	0.157	3.523	1.827	0.016	1.238	0.696	0.183	0
WOA (prop.)	33, 36	0.996	1.01	1.003	0.163	2.996	1.876	0.018	1.293	0.758	0.196	0
IWOA (conv.)	35, 24	0.999	1.009	1.003	0.152	4.67	2.79	0.014	3.863	1.32	0.082	0
WOA (conv.)	22, 33	0.999	1.01	1.004	0.133	4.69	3.06	0.02	4.244	1.587	0.109	0

Figures 10 and 11 present a comparison per bus for THD and PVUR, respectively, demonstrating that the proposed optimization methods significantly outperform the conventional approaches. The proposed IWOA method consistently yields the lowest THD and PVUR values across the system, demonstrating a clear advantage over the conventional WOA method and confirming its superior effectiveness in mitigating both the harmonic distortion and PVUR. A computational time analysis over 25 runs, as shown in Figure 12, reveals a clear performance trade-off. The proposed objective is slower than conventional due to the added complexity of the unbalanced and harmonic power flow calculations, while the IWOA is marginally slower than the WOA due to its enhanced search mechanism. This results in a performance hierarchy, with WOA (conventional) being the fastest and IWOA (proposed) being the most computationally demanding. This balance between the superior power quality optimization and higher computational cost is a significant consideration for practical, real-time implementation.

E. Statistical Analysis

To assess the reliability of the algorithm, a comparative analysis was performed across ten iterations using the proposed multi-objective function. Table VI and Figure 13 display the mean and standard deviation for the fitness values and convergence iterations for both WOA and IWOA. The analysis shows that IWOA exhibits higher efficiency and stability in comparison to the conventional WOA, as it converges at a rate that is nearly twice as fast (3.2 versus 6.1 average iterations) while maintaining greater consistency in performance (0.8717 versus 1.5579 standard deviation).

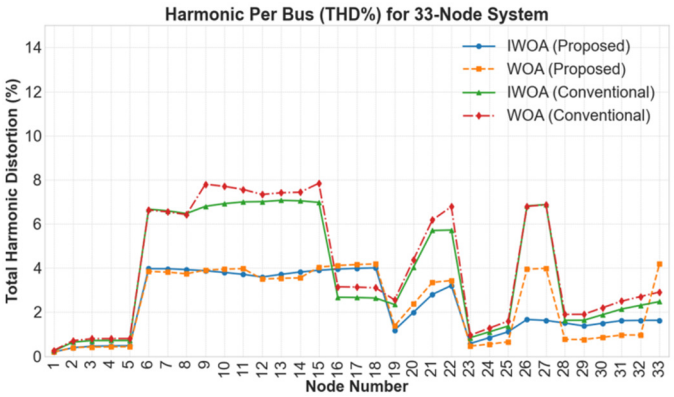

Fig. 10. Comparison of per-bus THD (%) for the tested algorithms and objectives.

Additionally, in terms of the solution quality, IWOA exhibited superior outcomes by attaining a higher mean fitness value compared to WOA (3.0745 versus 3.0881), underscoring its capacity to generate more precise and dependable optimization outcomes under diverse operating conditions. The findings, when considered collectively, confirm that the proposed IWOA not only accelerates the convergence process, but also ensures reliability and dependability. This, in turn, offers a more effective solution framework for addressing the

dynamic self-healing problem in smart microgrids. Ultimately, this contributes to enhanced resilience and improved operational reliability of the modern power distribution networks.

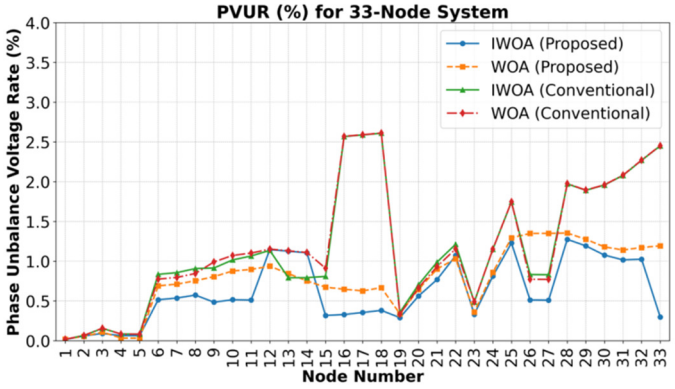

Fig. 11. Comparison of per-bus PVUR (%) for the tested algorithms and objectives.

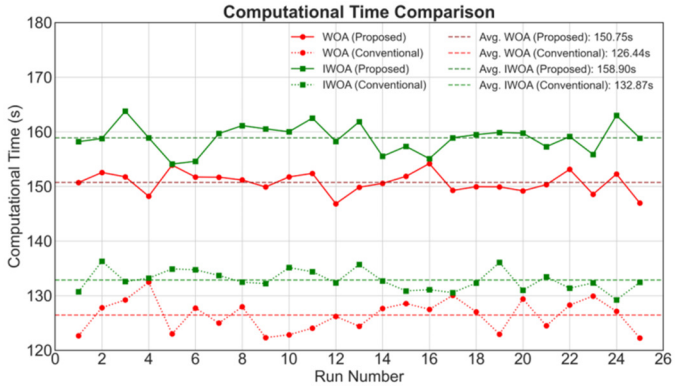

Fig. 12. Comparison of computational cost (s) for the tested algorithms and objectives.

TABLE VI. STATISTICAL COMPARISON OF IWOA AND WOA PERFORMANCE BASED ON FINAL FITNESS VALUE AND CONVERGENCE SPEED

Algorithm	Final fitness value		Convergence iteration	
	Mean	STD	Mean	STD
WOA	3.0881	0.0026	6.1	1.5779
IWOA	3.0745	0.0025	3.2	0.8717

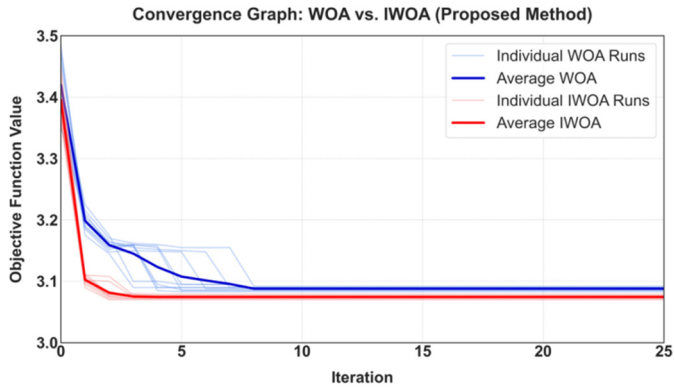

Fig. 13. Comparison of WOA and the proposed IWOA, showing average performance over 25 iterations.

VII. CONCLUSIONS

This study is a significant advancement in the dynamic self-healing of smart grids, providing several unique contributions to the field. The primary contributions of this work are: The novel adaptation of the Whale Optimization Algorithm (IWOA) was developed to address the discrete network reconfiguration problem under challenging unbalanced and harmonic conditions. This adaptation includes the integration of comprehensive power quality objectives, Total Harmonic Distortion (THD), and Phase Voltage Unbalance Rate (PVUR), directly into the optimization function alongside traditional metrics, ensuring a holistic approach to the system restoration. Additionally, the IWOA exhibits superior convergence and robustness, particularly in severe N-1, N-2, and N-3 fault scenarios. The algorithm's enhanced movement mechanism played a critical role in averting the premature convergence, a prevalent constraint of metaheuristics in complex power system applications. The results of the study showed that the IWOA exhibited a superior overall power quality in comparison to the standard WOA. Additionally, the IWOA exhibited a significant increase in efficiency, as evidenced by its nearly double convergence speed and greater solution stability. In addition, a weight sensitivity analysis validated the proposed balanced, multi-objective approach, demonstrating its superiority to the single-objective strategies that result in significant trade-offs. This research provides a validated framework for integrating power quality into self-healing strategies, offering a tool for maintaining the network integrity in modern smart grids. It is important to acknowledge the study's limitations and to incorporate practical system constraints, such as thermal limits, relay protection, line capacities, and communication delays, into future research.

ACKNOWLEDGMENT

This research was funded by the Direktorat Riset dan Pengabdian kepada Masyarakat – Institut Teknologi Sepuluh Nopember (ITS). The authors gratefully acknowledge the support provided.

REFERENCES

[1] H. Liang and X. Yin, "Self-Healing Control: Review, Framework, and Prospect," *IEEE Access*, vol. 11, pp. 79495–79512, 2023, https://doi.org/10.1109/ACCESS.2023.3298554.

[2] S. A. Arefifar, M. S. Alam, and A. Hamadi, "A Review on Self-Healing in Modern Power Distribution Systems," *Journal of Modern Power Systems and Clean Energy*, vol. 11, no. 6, pp. 1719–1733, Nov. 2023, https://doi.org/10.35833/MPCE.2022.000032.

[3] J. Dias Santos, F. Marques, L. P. Garcés Negrete, G. A. Andrêa Brigatto, J. M. López-Lezama, and N. Muñoz-Galeano, "A Novel Solution Method for the Distribution Network Reconfiguration Problem Based on a Search Mechanism Enhancement of the Improved Harmony Search Algorithm," *Energies*, vol. 15, no. 6, Jan. 2022, Art. no. 2083, https://doi.org/10.3390/en15062083.

[4] S. Punitha, N. P. Subramaniam, and P. A. D. Vimal Raj, "A comprehensive review of microgrid challenges in architectures, mitigation approaches, and future directions," *Journal of Electrical Systems and Information Technology*, vol. 11, no. 1, Dec. 2024, Art. no. 60, https://doi.org/10.1186/s43067-024-00188-4.

[5] B. Stojanović, T. Rajić, and D. Šošić, "Distribution network reconfiguration and reactive power compensation using a hybrid Simulated Annealing – Minimum spanning tree algorithm," *International Journal of Electrical Power & Energy Systems*, vol. 147,

May 2023, Art. no. 108829, https://doi.org/10.1016/j.ijepes.2022.108829.

[6] T.-Z. Ang, M. Salem, M. Kamarol, H. S. Das, M. A. Nazari, and N. Prabaharan, "A comprehensive study of renewable energy sources: Classifications, challenges and suggestions," *Energy Strategy Reviews*, vol. 43, Sept. 2022, Art. no. 100939, https://doi.org/10.1016/j.esr.2022.100939.

[7] M. Hasan *et al.*, "A critical review on control mechanisms, supporting measures, and monitoring systems of microgrids considering large scale integration of renewable energy sources," *Energy Reports*, vol. 10, pp. 4582–4603, Nov. 2023, https://doi.org/10.1016/j.egyr.2023.11.025.

[8] S. Dawn *et al.*, "Integration of Renewable Energy in Microgrids and Smart Grids in Deregulated Power Systems: A Comparative Exploration," *Advanced Energy and Sustainability Research*, vol. 5, no. 10, 2024, Art. no. 2400088, https://doi.org/10.1002/aesr.202400088.

[9] W. Li *et al.*, "Dynamic reconfiguration of active distribution network based on improved backtracking search algorithm," *Journal of Intelligent & Fuzzy Systems*, vol. 46, no. 1, pp. 1469–1480, Jan. 2024, https://doi.org/10.3233/JIFS-232993.

[10] S. Hou and W. Zhu, "Dynamic Reconfiguration Method of Photovoltaic Array Based on Improved HPSO Combined with Coefficient of Variation," *Electronics*, vol. 12, no. 12, Jan. 2023, Art. no. 2744, https://doi.org/10.3390/electronics12122744.

[11] E. Mahdavi, S. Asadpour, L. H. Macedo, and R. Romero, "Reconfiguration of Distribution Networks with Simultaneous Allocation of Distributed Generation Using the Whale Optimization Algorithm," *Energies*, vol. 16, no. 12, Jan. 2023, Art. no. 4560, https://doi.org/10.3390/en16124560.

[12] Y. Liu, S. Yang, D. Li, and S. Zhang, "Improved Whale Optimization Algorithm for Solving Microgrid Operations Planning Problems," *Symmetry*, vol. 15, no. 1, Jan. 2023, Art. no. 36, https://doi.org/10.3390/sym15010036.

[13] A. A. Chirani, "Network reconfiguration and optimal distributed generations allocation with whale optimizer algorithm," *Majlesi Journal of Electrical Engineering*, vol. 19, no. 1, pp. 1–12, Mar. 2025, https://doi.org/10.57647/j.mjee.2025.1901.04.

[14] H. Hizarci, O. Demirel, and B. E. Turkay, "Distribution network reconfiguration using time-varying acceleration coefficient assisted binary particle swarm optimization," *Engineering Science and Technology, an International Journal*, vol. 35, Nov. 2022, Art. no. 101230, https://doi.org/10.1016/j.jestch.2022.101230.

[15] N. Tu and Z. Fan, "IMODBO for Optimal Dynamic Reconfiguration in Active Distribution Networks," *Processes*, vol. 11, no. 6, June 2023, Art. no. 1827, https://doi.org/10.3390/pr11061827.

[16] U. Umar *et al.*, "Dual-Phase Parasitism SOS with Crossover Operator for Optimal Multi Single-Phase DG in Unbalance Distribution System," *International Journal of Intelligent Engineering and Systems*, vol. 15, no. 2, pp. 584–593, Apr. 2022, https://doi.org/10.22266/ijies2022.0430.52.

[17] H. K. Pujari, M. Rudramoorthy, R. Gopi R, S. Mishra, N. C. Alluraiah, and V. N. B., "Optimal reconfiguration, renewable DGs, and energy storage units' integration in distribution systems considering power generation uncertainty using hybrid GWO-SCA algorithms," *International Journal of Modelling and Simulation*, pp. 1–33, May 2024, https://doi.org/10.1080/02286203.2024.2363605.

[18] L. Abualigah *et al.*, "Whale optimization algorithm: analysis and full survey," in *Metaheuristic Optimization Algorithms*, L. Abualigah, Ed. Burlington, MA, USA: Morgan Kaufmann, 2024, pp. 105–115.

[19] K. Widarsono, A. Soeprijanto, and R. S. Wibowo, "Improved Whale Optimization Algorithm for Dynamic Optimal Power Flow with Renewable Energy Penetration," *Engineering, Technology & Applied Science Research*, vol. 15, no. 1, pp. 20379–20387, Feb. 2025, https://doi.org/10.48084/etasr.9662.

[20] C. Wang, C. Tu, S. Wei, L. Yan, and F. Wei, "MSWOA: A Mixed-Strategy-Based Improved Whale Optimization Algorithm for Multilevel Thresholding Image Segmentation," *Electronics*, vol. 12, no. 12, Jan. 2023, Art. no. 2698, https://doi.org/10.3390/electronics12122698.

[21] M. H. Nadimi-Shahraki, H. Zamani, Z. Asghari Varzaneh, and S. Mirjalili, "A Systematic Review of the Whale Optimization Algorithm: Theoretical Foundation, Improvements, and Hybridizations," *Archives of Computational Methods in Engineering*, vol. 30, no. 7, pp. 4113–4159, Sept. 2023, https://doi.org/10.1007/s11831-023-09928-7.

[22] F. A. Haidar Fayumi, R. S. Wibowo, and D. F. Uman Putra, "Multi-Objective Dynamic Network Reconfiguration Considering Voltage Stability and Integration of Distributed Energy Sources Using SPSO-IPOPT," in *2024 International Seminar on Intelligent Technology and Its Applications (ISITIA)*, Mataram, Indonesia, July 2024, pp. 560–565, https://doi.org/10.1109/ISITIA63062.2024.10668375.

[23] M. N. Hakim *et al.*, "Optimal Reconfiguration of Distribution Network With Photovoltaic Using Binary Particle Swarm Optimization Considering Voltage Stability Index," in *2024 International Seminar on Intelligent Technology and Its Applications (ISITIA)*, Mataram, Indonesia, July 2024, pp. 53–58, https://doi.org/10.1109/ISITIA63062.2024.10667848.